



## Removal of pharmaceutically active substance ibuprofen from aqueous solution using TiO<sub>2</sub>/ZSM-5 zeolite hybrid photocatalysts

SRNA J. STOJANOVIĆ<sup>1</sup>, MARIJA Z. RISTIĆ<sup>2</sup>, DANINA R. KRAJIŠNIK<sup>3</sup>, VLADISLAV A. RAC<sup>4</sup> and LJILJANA S. DAMJANOVIĆ-VASILIĆ<sup>1\*</sup>

<sup>1</sup>University of Belgrade – Faculty of Physical Chemistry, Studentski trg 12–16, 11000 Belgrade, Serbia, <sup>2</sup>University of Belgrade – ICTM, Department of Catalysis and Chemical Engineering, Njegoševa 12, 11000 Belgrade, Serbia, <sup>3</sup>University of Belgrade – Faculty of Pharmacy, Vojvode Stepe 450, 11221 Belgrade, Serbia, and <sup>4</sup>University of Belgrade-Faculty of Agriculture, Nemanjina 6, 11080 Belgrade, Serbia

(Received 18 October, revised 9 November, accepted 1 December 2024)

**Abstract:** The removal of pharmaceutically active substance ibuprofen (IBU) from aqueous solution was studied using TiO<sub>2</sub>/ZSM-5 zeolite hybrid photocatalysts synthesized from 20 wt. % TiO<sub>2</sub> P25 nanoparticles and ZSM-5 zeolites with different Si/Al ratio (11.5, 15, 25, 40 and 140). The hybrid materials were prepared by a simple and economic ultrasound assisted solid-state dispersion method and characterized by X-ray powder diffraction, Fourier transform infrared spectroscopy and ultraviolet-visible diffuse reflectance spectroscopy. Among them, the hybrid photocatalyst containing TiO<sub>2</sub> and ZSM-5 zeolite with a Si/Al = 40 (denoted as TZ(40)) showed the highest removal efficiency, achieving 85 % IBU removal after 80 min under UV irradiation. The optimal condition for the removal of IBU from deionized water was found to be at a natural pH 4.5. Moreover, the removal of IBU from bottled drinking water in the presence of TZ(40) hybrid material was tested. Only 32 % IBU removal was achieved because change in pH value of reaction suspension decreased efficiency of IBU removal.

**Keywords:** ibuprofen; photocatalytic degradation; titanium dioxide; ZSM-5 zeolite.

### INTRODUCTION

The pharmaceuticals represent an important group of emerging pollutants that cause major concern in recent years. These compounds are widely used in human medicine, veterinary medicine and aquaculture.<sup>1</sup> They often enter the aquatic ecosystems through various sources such as municipal wastewater, inap-

\* Corresponding author. E-mail: ljiljana@ffh.bg.ac.rs  
<https://doi.org/10.2298/JSC241018098S>

ropriate disposition of expired medicines, human and animal excretions in livestock farming.<sup>2,3</sup> Currently, numerous pharmaceutically active substances can be found in various water sources at concentrations ranging from ng L<sup>-1</sup> to µg L<sup>-1</sup>. These pollutants are widespread in the environment because the traditional methods for water treatment are insufficiently effective for their removal.<sup>4,5</sup> Long-term exposure to these compounds can cause harmful effects on aquatic organisms and human beings.<sup>1</sup>

Among the most widely used pharmaceuticals in the world are non-steroidal anti-inflammatory drugs (NSAIDs), such as ibuprofen (IBU), which are often detected in the environment.<sup>6</sup> In a study conducted in Serbia, alongside pharmaceuticals such as diclofenac, codeine, valsartan, acetaminophen and carbamazepine derivatives, IBU was detected in municipal wastewater at a concentration of 20.1 µg L<sup>-1</sup>.<sup>7</sup> Similarly, in Tehran, Iran, a study analysed NSAIDs and found that IBU was the most prevalent, with concentrations of 1.05 µg L<sup>-1</sup> in municipal wastewater influents and lower levels in tap water, including the maximum values of 47 ng L<sup>-1</sup> for IBU.<sup>5</sup>

Given the pressing need for development of technologies for removal of these contaminants, the methodologies involving advanced oxidation processes (AOPs) which are known to be very effective towards mineralization of organic compounds, offer a promising solution. Among semiconductor materials, titanium dioxide has been investigated for the removal of IBU, demonstrating its effectiveness in degrading this pharmaceutical.<sup>8,9</sup> Its unique properties, such as high stability, large specific surface area, non-toxicity, and high activity, make it an effective material for degrading organic pollutants.<sup>10</sup>

However, because of the tendency of TiO<sub>2</sub> nanoparticles to agglomerate and the high costs associated with filtration, certain constraints exist, regarding its widespread practical implementation. To address these challenges, the immobilization of TiO<sub>2</sub> nanoparticles on various supports with high surface area (such as zeolites, clay, carbon, etc.) has been proposed, which could enhance the removal process and facilitate easier recovery of the photocatalytic material from treated water.<sup>11–13</sup>

Zeolites are microporous hydrated aluminosilicates with a three-dimensional framework consisting of tetrahedral SiO<sub>4</sub> and AlO<sub>4</sub> units, with the silicon to aluminium ratio significantly influencing their structure and properties like hydrophobicity, acidity, catalytic activity, thermal and hydrothermal stability.<sup>14</sup> Although zeolites are known for their great adsorption properties and are widely used in the studies related to removal of different pharmaceuticals,<sup>15</sup> these materials have also proven to be appropriate support for semiconductor photocatalysts such as TiO<sub>2</sub>, improving their performance in pollutant degradation.<sup>16</sup> Furthermore, the zeolites' transparency above 240 nm makes them ideal for UV light excitation of TiO<sub>2</sub>.<sup>16</sup>

The materials based on TiO<sub>2</sub> and zeolites have been investigated for the removal of pharmaceuticals such as acetaminophen, codeine and cefazolin from aquatic environment.<sup>17,18</sup> In our previous study the removal of atenolol, a  $\beta$ -blocker, was investigated using nanosized TiO<sub>2</sub> and various zeolites, with the highest removal efficiency achieved by TiO<sub>2</sub>/ZSM-5 zeolite hybrid photocatalyst.<sup>19</sup> Only few studies assessed the removal of IBU using Pd-TiO<sub>2</sub>/ZSM-5 catalyst<sup>20</sup> and UV/H<sub>2</sub>O<sub>2</sub>/zeolite–titannate photocatalyst system.<sup>21,22</sup>

The aim of this study was to investigate the photocatalytic performance of TiO<sub>2</sub>/ZSM-5 zeolite hybrid photocatalysts for the removal of IBU from aqueous solution. The synthetic ZSM-5 zeolite, used as one component of hybrid material, consists of interconnected channels with 10-membered openings ( $5.1\text{ \AA} \times 5.5\text{ \AA}$  and  $5.3\text{ \AA} \times 5.6\text{ \AA}$ ). These channels intersect and form the opening with size of approximately  $8.5\text{--}9.0\text{ \AA}$ .<sup>23</sup> The commercial nanoparticles TiO<sub>2</sub> P25 was used as another component. The hybrid photocatalysts were prepared using a facile and economical ultrasound assisted solid-state dispersion (USSD) method and characterized by X-ray powder diffraction (XRPD), Fourier transform infrared (FTIR) spectroscopy and ultraviolet–visible diffuse reflectance (UV–Vis DR) spectroscopy. The influence of different Si/Al ratio of ZSM-5 zeolite in the prepared TiO<sub>2</sub>/ZSM-5 hybrid materials on the IBU removal process was evaluated, along with the effects of varying pH values. Furthermore, the influence of different water matrix such as commercial bottled drinking water and water spiked with bicarbonate ions to the removal of IBU were also studied.

## EXPERIMENTAL

### Materials

IBU was provided by the pharmaceutical company Galenika a.d., Serbia. This active substance was of pharmacopoeial (Ph. Eur.) grade. The structural formula of IBU is shown in Fig. S-1 of the Supplementary material to this paper. The ZSM-5 zeolites with Si/Al ratio of 11.5, 15, 25, 40 and 140 from Zeolyst were used. TiO<sub>2</sub> nanoparticles ( $\geq 99.5\%$ , Evonik Aerioxide® TiO<sub>2</sub> P25, primary particle size of 21 nm), were obtained from Aldrich. The other chemicals used in this study included ethanol ( $> 99.8\%$ , Fisher Scientific), sodium hydrogen carbonate (NaHCO<sub>3</sub>,  $>99.5\%$ , Lachema), sodium hydroxide (NaOH,  $\geq 99\%$ , Emsure®, Merck), hydrochloric acid (35 %, p. a., Lachner) and KBr ( $\geq 99.5\%$ , Emsure®, Merck).

### Preparation of TiO<sub>2</sub>/ZSM-5 zeolite materials

Beside ZSM-5 zeolite with Si/Al = 15 which was purchased in hydrogen form, all other used ZSM-5 zeolites were converted from their ammonium to hydrogen form by calcination at 500 °C for 5 h. ZSM-5 zeolites were denoted as Z(11.5), Z(15), Z(25), Z(40) and Z(140), where Z represents the used zeolite, and the number in parentheses indicates Si/Al ratio. TiO<sub>2</sub>/ZSM-5 zeolite hybrid photocatalysts were prepared using an ultrasound assisted solid-state dispersion (USSD) method described in our earlier work.<sup>24</sup> A 20 wt. % of TiO<sub>2</sub> was thoroughly mixed with the starting zeolite in an agate mortar using a pestle, and the mixture was ultrasonically dispersed in ethanol (10:1 ethanol (mL) to solid powder (g) ratio) for 15 min at 80 °C using an ultrasonic bath (Bandelin Sonorex RK52H, 35 Hz and 240 W). The

samples were subsequently dried at 80 °C and then calcined in air at 500 °C for 5 h. The prepared samples were labelled as TZ(11.5), TZ(15), TZ(25), TZ(40) and TZ(140), where T represents TiO<sub>2</sub> P25 and Z(11.5) the zeolite and its Si/Al ratio.

#### Methods

The XRPD patterns of the TiO<sub>2</sub> P25, starting zeolites and TiO<sub>2</sub>/ZSM-5 zeolite hybrid materials were recorded using a Rigaku Ultima IV diffractometer in Bragg–Brentano geometry. CuK $\alpha$  radiation ( $\lambda = 1.54178 \text{ \AA}$ ) was used, with measurements taken over  $2\theta$  range from 4 to 50°, using a step of 0.020° and an acquisition rate of 1° min<sup>-1</sup>.

FTIR spectra of all investigated materials were recorded using a Thermo Scientific Nicolet Avatar 370 FTIR spectrophotometer. The measurements were conducted in the range of 4000–400 cm<sup>-1</sup> with a resolution of 4 cm<sup>-1</sup> and 64 acquisitions. KBr pellets were prepared by mixing 1.5 mg of the sample with 150 mg of KBr.

UV–Vis DR spectra were obtained using an Agilent Cary UV–Vis NIR 5000 spectrophotometer equipped with an integration sphere in the range from 200 – 600 nm, with a data interval of 1 nm and a scan rate of 600 nm min<sup>-1</sup>. Polytetrafluoroethylene (PTFE) was used as a white reference standard for measuring base line.

#### Photodegradation procedure

The photocatalytic performance of the starting materials and TiO<sub>2</sub>/ZSM-5 zeolite hybrid materials was evaluated in a 50 mL glass reactor. A glass reactor had a water-cooling jacket which was used to retain room temperature (25±2 °C). The experiments were carried out using 40 mL of aqueous solution of IBU ( $C_0 = 30 \text{ mg L}^{-1}$ ) with 1 g L<sup>-1</sup> of catalyst under constant stirring and illumination from a HPR 125 Philips high vapour pressure mercury lamp (125 W; emission bands in the UV region at 313, 334.2, 365.5 and 390.6 nm, with the maximum emission at 365.5 nm). The investigated concentration of IBU was higher than those usually detected in wastewaters, with the aim of detecting changes in the process within measurable time scale with used analytical technique.

The lamp was positioned at a distance of 25 cm from the experimental suspension. To reach adsorption–desorption equilibrium, the suspensions were stirred for 15 min in the dark. At predetermined time intervals, 1 mL aliquots were withdrawn and centrifuged at 12,000 rpm for 15 min to separate the particles from the supernatant. The changes of IBU ( $\lambda_{\text{max}} = 221 \text{ nm}$ ) concentrations in the supernatant were determined from absorbance spectra recorded on a Thermo Scientific Evolution 220 UV–Vis spectrophotometer in the range from 200 to 400 nm. The photocatalytic experiments were conducted in triplicate to confirm the reproducibility of the data and the mean of the acquired results is presented together with the standard deviation (as error bars in the figures).

Furthermore, to evaluate the practical applicability of the most efficient hybrid photocatalysts for the removal of IBU, photocatalytic experiments were conducted in bottled drinking water. For these experiments, IBU was dissolved in commercial bottled water with the following composition: HCO<sub>3</sub><sup>-</sup> = 42.7 mg L<sup>-1</sup>, NO<sub>3</sub><sup>-</sup> = 1.46 mg L<sup>-1</sup>, SO<sub>4</sub><sup>2-</sup> = 5.2 mg L<sup>-1</sup>, Cl<sup>-</sup> = < 1 mg L<sup>-1</sup>, Ca<sup>2+</sup> = 9.6 mg L<sup>-1</sup>, Mg<sup>2+</sup> = 0.82 mg L<sup>-1</sup>, Na<sup>+</sup> = 2.7 mg L<sup>-1</sup>, K<sup>+</sup> < 1 mg L<sup>-1</sup>, and conductivity = 69.5  $\mu\text{S cm}^{-1}$  and pH 7.5. Subsequently, to determine the influence of bicarbonate anions on the photocatalytic activity of TiO<sub>2</sub>/ZSM-5 zeolite hybrid photocatalysts, aqueous solution of IBU was spiked with HCO<sub>3</sub><sup>-</sup> = 42.7 mg L<sup>-1</sup>.

For the studies of pH influence on the removal of IBU from aqueous solution, the pH values of solutions were adjusted by adding HCl or NaOH. The pH measurements were conducted using a PC5 multiparameter tester (XS Instruments).

## RESULTS AND DISCUSSION

*XRPD analysis*

The XRPD patterns of  $\text{TiO}_2$  P25, the starting ZSM-5 zeolites and  $\text{TiO}_2$ /ZSM-5 zeolite hybrid materials are shown in Fig. 1. The XRPD pattern of  $\text{TiO}_2$  P25 revealed reflections corresponding to the anatase phase ( $2\theta$  of 25.3, 37.0, 37.8, 38.6 and 48.1°; JCPDS 89-4921) and the rutile phase ( $2\theta$  of 27.4 and 36.1°; JCPDS 89-8304). The XRPD patterns of all starting ZSM-5 zeolites exhibited the characteristic reflections of the MFI structure at  $2\theta$  of 7.9, 8.9, 23.9, 29.9°.<sup>25</sup> In the diffractograms of  $\text{TiO}_2$ /ZSM-5 zeolite hybrid materials, the reflections from both ZSM-5 zeolite and  $\text{TiO}_2$  phases (anatase:  $2\theta$  of 25.3, 37.8 and 48.1°; JCPDS 89-4921 and rutile:  $2\theta = 27.4^\circ$ ; JCPDS 89-8304) are detected. These results confirm the successful loading of  $\text{TiO}_2$  nanoparticles on the starting zeolites and the preservation of zeolite structure.

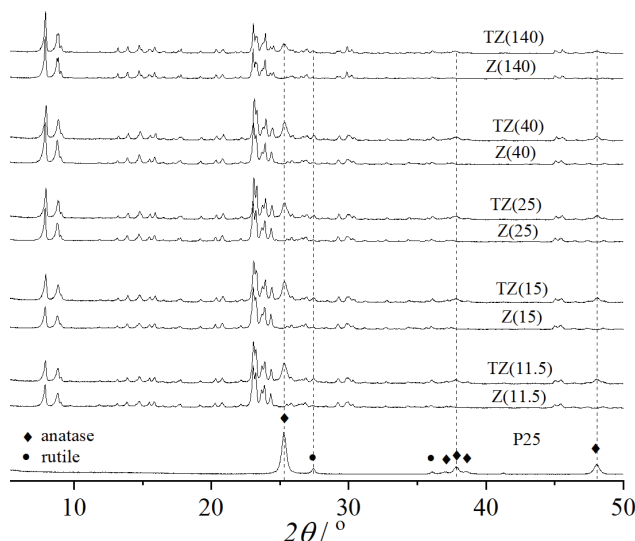


Fig. 1. XRPD patterns of  $\text{TiO}_2$  P25, the starting zeolites and  $\text{TiO}_2$ /ZSM-5 zeolite hybrid photocatalysts. Vertical dashed lines are at 25.3, 27.4, 37.8 and 48.1°.

*FTIR spectroscopy*

The FTIR spectra of  $\text{TiO}_2$  P25, the starting ZSM-5 zeolites and  $\text{TiO}_2$ /ZSM-5 zeolite hybrid materials are shown in Fig. 2. In these spectra, the characteristic bands originating from the vibrations of ZSM-5 zeolite framework are present. The band at  $\sim 453 \text{ cm}^{-1}$  corresponds to the bending vibrations of T–O bonds (T is Si, Al). The band positioned at  $\sim 545 \text{ cm}^{-1}$  is attributed to the external stretching vibrations of double 6-member rings (D6R), while the band at  $\sim 794 \text{ cm}^{-1}$  corresponds to the external symmetric stretching vibrations of T–O bonds.<sup>24</sup> The band

at  $\sim 1095\text{ cm}^{-1}$  is related to the asymmetric stretching vibrations of T–O–T bonds and the band at  $\sim 1221\text{ cm}^{-1}$  is attributed to the external asymmetric stretching vibrations of T–O–T bonds.<sup>26</sup>

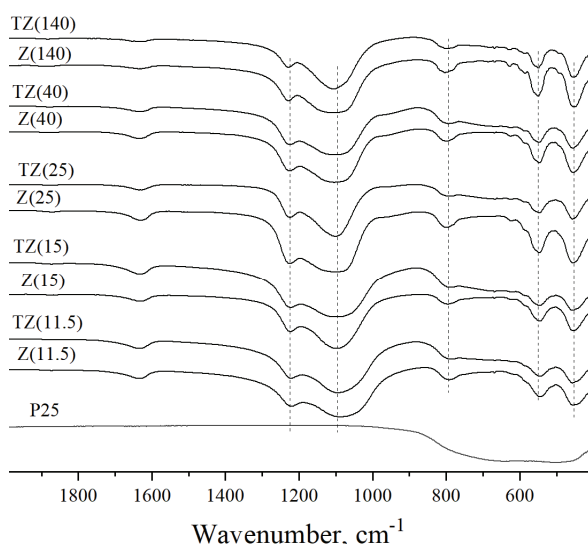


Fig. 2. FTIR spectra of  $\text{TiO}_2$  P25, starting zeolites and  $\text{TiO}_2/\text{ZSM-5}$  zeolite hybrid photocatalysts. Vertical dashed lines are at  $1221, 1095, 794, 545$  and  $453\text{ cm}^{-1}$ .

The FTIR spectra of  $\text{TiO}_2$  P25 is characterized by broad band below  $1000\text{ cm}^{-1}$  consisting of two signals originating from Ti–O and Ti–O–Ti stretching vibrations.<sup>27</sup> In the case of all investigated hybrid materials, a broadening of the bands in the  $400\text{--}600\text{ cm}^{-1}$  range was observed, attributed to the overlapping of the bands originating from the zeolite and  $\text{TiO}_2$ .

Since there were no significant changes in the FTIR spectra of the starting zeolites and  $\text{TiO}_2/\text{ZSM-5}$  zeolite hybrid materials, it can be concluded that the zeolite structure was preserved, which aligns with the XRD results. The absence of a band present at about  $960\text{ cm}^{-1}$  in FTIR spectra of  $\text{TiO}_2/\text{ZSM-5}$  zeolite hybrid materials, typically associated with the asymmetric stretching vibration of Ti–O–Si bonds, suggests that Ti species are immobilized on the external surface of the zeolite, rather than being incorporated into the internal structure.<sup>28</sup>

#### *UV–Vis DR spectroscopy*

The light absorption properties of  $\text{TiO}_2/\text{ZSM-5}$  zeolite hybrid materials were evaluated using UV–Vis DR spectroscopy. The obtained results together with the UV–Vis DR spectra of the starting materials are presented in Fig. 3. As observed from the spectra, all  $\text{TiO}_2/\text{ZSM-5}$  zeolite hybrid materials exhibited characteristic absorption in the UV region, corresponding to the optical absorbance ability of

TiO<sub>2</sub> nanoparticles dispersed on the ZSM-5 zeolites. No significant shift in the absorption edges was observed when comparing the TiO<sub>2</sub> P25 and the TiO<sub>2</sub>/ZSM-5 zeolite hybrid photocatalysts which indicate that the optical properties of TiO<sub>2</sub> were preserved after the preparation of these materials. Furthermore, these results confirm the successful loading of TiO<sub>2</sub>, which is consistent with the XRPD and FTIR spectroscopy findings.

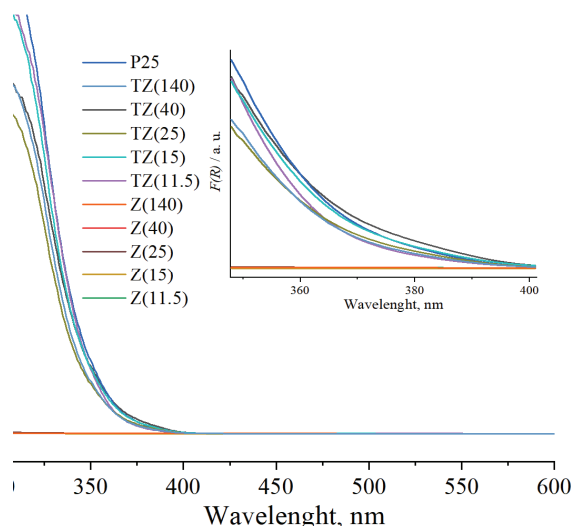


Fig. 3. UV–Vis DR spectra of TiO<sub>2</sub> P25, starting zeolites and TiO<sub>2</sub>/ZSM-5 zeolite hybrid photocatalysts.

*The efficiency of TiO<sub>2</sub>/ZSM-5 zeolite hybrid photocatalysts for IBU removal from aqueous solution*

The results of photocatalytic removal of IBU from aqueous solution in the presence of starting ZSM-5 zeolites with different Si/Al ratios and TiO<sub>2</sub>/ZSM-5 zeolite hybrid materials are shown in Fig. 4. IBU has two characteristic bands with absorption maxima at 221 nm and 264 nm in the UV–Vis spectra, related to benzene ring.<sup>8</sup> In this study, the concentration of IBU was monitored based on absorbance at 221 nm.

Initially, the photolysis of IBU was investigated, and the results showed that there were no changes in the UV–Vis spectra after 120 min of UV irradiation (Fig. S-2 of the Supplementary material) demonstrating that IBU remains stable under the investigated conditions. Subsequently, the adsorption in the dark and photocatalytic ability of the starting ZSM-5 zeolites with different Si/Al ratio was investigated, and obtained results are presented in Fig. 4a. The findings reveal that during 15 min of stirring in the dark, the concentration of IBU decreased due to adsorption on the initial zeolites. Upon turning on the lamp, the IBU concen-

tration remains unchanged, confirming that ZSM-5 zeolites do not act as photocatalysts.

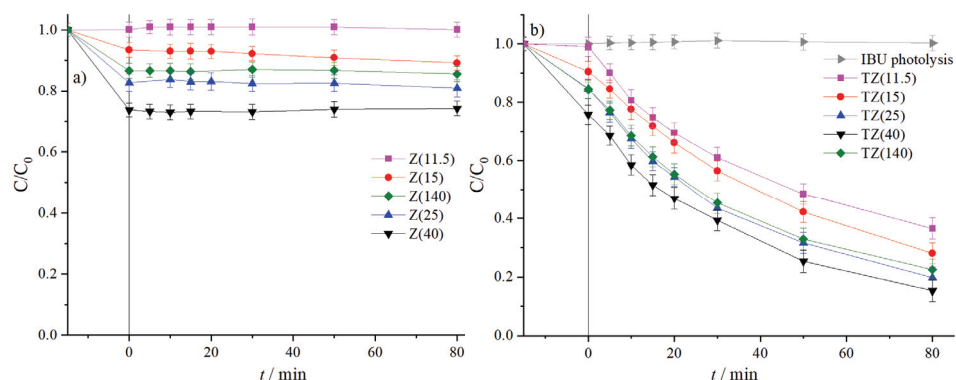


Fig. 4. Adsorption in the dark and photodegradation of IBU in the presence of: a) starting ZSM-5 zeolites with different Si/Al ratio and b)  $\text{TiO}_2/\text{ZSM-5}$  zeolite hybrid photocatalysts with 20 wt. % of  $\text{TiO}_2$ ; photolysis of IBU is shown for comparison. (Experimental conditions:  $C_0 = 30 \text{ mg L}^{-1}$ ,  $1 \text{ g L}^{-1}$  catalyst; initial pH values of IBU solution in the presence of pure zeolites and hybrid photocatalysts are similar varying between 4.0 and 4.3).

The results showed (Fig. 4a) that Z(11.5), the most acidic zeolite, did not adsorb IBU. An increase in the Si/Al ratio led to higher IBU adsorption, with Z(15) removing 11, Z(25) 19 and Z(40) removing 26 %, which is in accordance with literature, *i.e.*, increase of Si/Al ratio results in an increase in hydrophobicity for the same zeolite framework type and consequently in higher adsorption of organic micro-pollutants.<sup>29</sup> Despite having the highest Si/Al ratio, Z(140) exhibited a decrease in IBU adsorption, achieving only the removal of 15 %, which can be explained by competition between water and IBU molecules for the same adsorption sites with increased hydrophobicity.<sup>29</sup>

The photodegradation of IBU in the presence of  $\text{TiO}_2/\text{ZSM-5}$  zeolite hybrid photocatalysts is shown in Fig. 4b. Among the  $\text{TiO}_2/\text{ZSM-5}$  zeolite hybrid materials, TZ(40) was the most efficient, removing 85 % of IBU after 80 min of irradiation. The UV–Vis spectra of IBU photodegradation in the presence of TZ(40) hybrid photocatalyst after 5, 10, 15, 20, 30, 50 and 80 min of UV irradiation are shown in Fig. S-3a of the Supplementary material. This was followed by TZ(25), which removed 80 % of IBU, TZ(140) 77 % of IBU, TZ(15) 72 % of IBU and TZ(11.5) 64 % of IBU. For TZ(11.5), the removal of IBU from aqueous solution was achieved solely through photocatalytic degradation. In contrast, for the other  $\text{TiO}_2/\text{ZSM-5}$  zeolite hybrid materials, the removal resulted from a combination of adsorption and photocatalytic degradation, which enhanced the overall removal efficiency.

The kinetics of photocatalytic IBU degradation can be modelled using the Langmuir–Hinshelwood equation, which at low concentration is converted to pseudo-first-order kinetic model represented by the following equation:  $\ln(C_0/C) = k_{app}t$ , where  $k_{app}$  is the rate constant,  $C_0$  is the initial concentration of IBU,  $C$  is the concentration at different irradiation time  $t$ .<sup>30</sup> The pseudo-first-order rate constants were determined as slope from linear plot of  $\ln(C_0/C)$  versus irradiation time ( $t$ ) for investigated hybrid photocatalysts and the results are shown in Table I. Besides the highest IBU adsorption, the highest rate constant has been determined for TZ(40). Thus, the combined adsorption and photocatalytic efficiency result in the highest removal efficiency for IBU using TZ(40).

TABLE I. Values of rate constant determined based on fit of UV–Vis experimental data to pseudo-first-order kinetic model

Sample	$k_{app}$ / min <sup>-1</sup>	$R^2$
TZ(11.5)	0.0135±0.0007	0.9911
TZ(15)	0.0151±0.0003	0.9982
TZ(25)	0.0188±0.0007	0.9988
TZ(40)	0.0209±0.0006	0.9957
TZ(140)	0.0177±0.0007	0.9948

For comparison, in the presence of pure TiO<sub>2</sub> P25 nanoparticles, using the amount of TiO<sub>2</sub> which corresponded to 20 wt. % of catalyst loading in composites, band at 221 nm in UV spectra (Fig. S-4 of the Supplementary material) strikingly disappears after 10 min of irradiation proving fast photocatalytic degradation of IBU, whereas intensity of band at 260 nm increases for 20 min and then decreases. According to the literature, band at 260 nm originates from the formation of temporary photodegradation products which can be degraded with prolonged irradiation.<sup>8,22</sup> It is interesting to note that band at 260 nm has significantly smaller intensity when TZ(40) is used as photocatalyst compared to pure TiO<sub>2</sub> (Figs. S-3a and S-4), indicating lower concentration of photodegradation products in the reaction mixture, which can be explained either by different degradation mechanism or by adsorption of degradation products by TZ(40).

Among limited number of studies investigating removal of IBU form aqueous solution in the presence of hybrid photocatalysts based on zeolites, Pd-TiO<sub>2</sub>/ZSM-5 catalyst achieved 80 % removal of IBU after 300 min of UVC irradiation (with low power) using a lower initial IBU concentration of 10 ppm and a smaller catalyst dose of 0.17 g L<sup>-1</sup>,<sup>20</sup> whereas TZ(40), catalyst dose 1 g L<sup>-1</sup>, achieved higher removal efficiency in a much shorter time (80 min) despite the higher IBU concentration (30 mg L<sup>-1</sup>). Similarly, an another study reported the highest removal efficiency of 97.5 % of IBU using zeolite-titanate photocatalyst prepared by sol–gel method (under experimental conditions: IBU concentration 100 mg L<sup>-1</sup>, 6W UVC lamp, pH 7, 0.7 mL H<sub>2</sub>O<sub>2</sub>, catalyst dose 1.67 g L<sup>-1</sup> 100

min sonication).<sup>21</sup> In a follow-up study, the zeolite-titanate photocatalyst was tested for IBU removal from different media and achieved 77.82 % removal of IBU from tap water and 96.48 % of IBU from deionized water (under experimental conditions: IBU concentration 100 mg L<sup>-1</sup>, pH 5, 0.05 mM H<sub>2</sub>O<sub>2</sub>, 1 g L<sup>-1</sup> catalyst, 6W UVC, 100 min sonication).<sup>22</sup> Unlike these studies, where chemicals such as H<sub>2</sub>O<sub>2</sub> are used as well as sonication, TZ(40) achieved comparable performance without such enhancements. This highlights its superior efficiency and the potential for cost-effective practical applications in water purification. Moreover, combined TiO<sub>2</sub> and zeolites result in an efficient hybrid photocatalyst which can be easily separated from aqueous media. In addition, in our previous work the reusability of TZ(40) was tested, revealing that TiO<sub>2</sub> is firmly immobilized on zeolite and that the calcination process can recover initial activity of TZ(40).<sup>19</sup>

Since the TZ(40) demonstrated the highest efficiency among the investigated hybrid photocatalysts for the removal of IBU, it was further tested.

#### *Influence of pH on the removal of IBU from aqueous solution*

The pH of the solution is a crucial factor that can significantly influence the efficiency of pollutant removal during heterogeneous catalysis, as it affects both the surface properties of the catalyst and the ionization state of the pollutants.<sup>4,31</sup> Therefore, the removal process of IBU from aqueous solution was investigated at different pH values in the presence of TZ(40) and the results are shown in Fig. 5. The natural pH of the IBU aqueous solution was 4.3, and the pH of the reaction suspension with hybrid material was 4.5. As reported in the literature, the pK<sub>a</sub> of IBU is 4.4.<sup>32</sup> At pH values below pK<sub>a</sub>, IBU will predominantly exists in its molecular (protonated) form, while at pH values above pK<sub>a</sub>, it will be present in its deprotonated form (IBU<sup>-</sup>).<sup>33</sup> In our previous work, the isoelectric point of TZ(40) has been determined to be at pH 3.3.<sup>19</sup> Meaning, at this pH the surface charge of TZ(40) is neutral, while at pH values higher than 3.3 the surface becomes negatively charged, and at pH values lower than 3.3 it becomes positively charged.

The highest removal percentage of IBU (85 %) was achieved at the natural pH of suspension. However, when the pH was adjusted to 3, 7 and 10, the removal efficiency decreased to 70, 29 and 27 %, respectively. Although at pH 3 the adsorption in the dark was higher (32 %) compared to the adsorption at natural pH (24 %), the photodegradation was reduced. At pH 7 as well as at pH 10, there was no adsorption of IBU in the dark in the presence of hybrid material. These findings can be explained by the surface charge interactions between the hybrid material and IBU at different pH values. At the alkaline conditions (pH 10) and at the neutral conditions (pH 7) the surface of TZ(40) is negatively charged, and IBU is predominantly in its deprotonated form (IBU<sup>-</sup>), which leads to the electro-

static repulsion between the catalyst and the pollutant. This repulsion likely explains the absence of adsorption in the dark and the reduced photocatalytic degradation. In the case of acidic conditions (pH 3), the surface of TZ(40) becomes positively charged, while IBU exists in its neutral, molecular form. The lack of significant interaction between the positively charged surface and neutral IBU results in lower photocatalytic degradation, despite the increased adsorption observed in the dark.

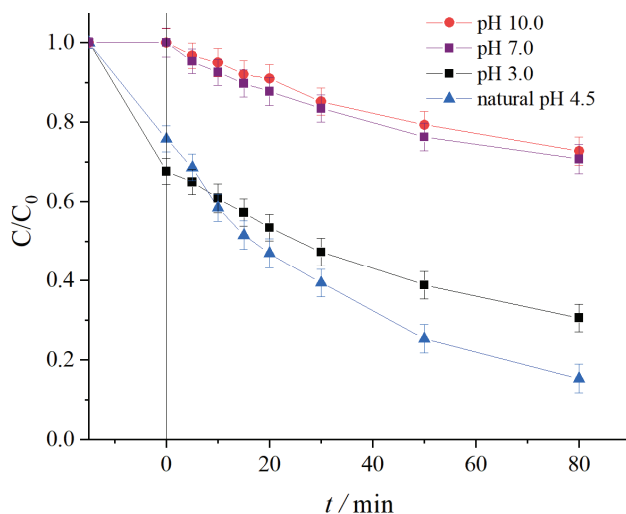


Fig. 5. Effect of pH on IBU removal in the presence of TZ(40) hybrid photocatalyst.  
(Experimental conditions:  $C_0 = 30 \text{ mg L}^{-1}$ ,  $1 \text{ g L}^{-1}$  catalyst).

Similar findings were observed in a study where the removal of IBU was less efficient at pH 3 and 9 compared to pH 7, using  $\text{TiO}_2$  P25 catalyst (isoelectric point: 6) under UV–Vis irradiation, with  $10 \text{ mg L}^{-1}$  of IBU and  $20 \text{ mg L}^{-1}$  of catalyst.<sup>8</sup>

#### *Influence of water media on the removal of IBU*

The effectiveness of TZ(40) hybrid material for the removal of IBU in bottled drinking water was also evaluated, considering its potential for practical application. The results of IBU removal in the presence of TZ(40) hybrid material in different water media are shown in Fig. 6.

After 80 min of irradiation in the presence of TZ(40), 85 % of IBU was successfully removed. In contrast, the removal efficiency of IBU was significantly reduced in bottled drinking water, achieving only 32 % removal. This decrease can be attributed to the presence of various inorganic ions commonly found in drinking water, which may interfere with the photocatalytic degradation. Notably, the bicarbonate ions are known to act as radical scavengers, reacting with

hydroxyl radicals to form less reactive carbonate radicals, thereby reducing the availability of reactive oxygen species needed for the degradation of organic pollutants.<sup>34,35</sup> Given that bicarbonate ions were present at the highest concentration among other ions in used bottled drinking water, an additional experiment was conducted, where IBU was dissolved in deionized water with bicarbonates added at the same concentration as in the bottled water. The results showed that the presence of bicarbonate ions significantly slowed the degradation process. However, the addition of bicarbonate ions changed pH of reaction suspension from 4.5 (IBU solution in deionized water in the presence of TZ(40)) to 7. As shown in Fig. 5, decrease in the IBU removal has been obtained without bicarbonate ions in this reaction suspension at pH 7. Thus, the decrease in the IBU removal is due to the change of pH of the reaction suspension, not the presence of bicarbonates. Consequently, a longer period of irradiation would be necessary for the IBU removal from drinking water in the presence of TZ(40).

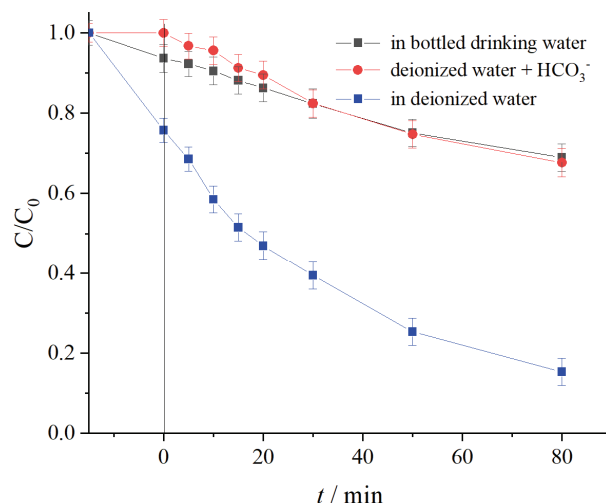


Fig. 6. Removal of IBU in the presence of TZ(40) hybrid material in deionized water, bottled drinking water and deionized water with addition of bicarbonates ( $42.7 \text{ mg L}^{-1}$ ). (Experimental conditions:  $C_0 = 30 \text{ mg L}^{-1}$ ,  $1 \text{ g L}^{-1}$  catalyst; initial pH values before irradiation of reaction suspensions were: 4.5 in deionized water; 7 in deionized water +  $\text{HCO}_3^-$ ; 6.4 in bottled drinking water).

#### CONCLUSION

This study demonstrated the successful preparation of  $\text{TiO}_2/\text{ZSM-5}$  zeolite hybrid photocatalysts based on  $\text{TiO}_2$  P25 nanoparticles and ZSM-5 zeolites with different Si/Al ratio, using a facile ultrasound assisted solid-state dispersion method. The photocatalytic results showed that the hybrid material containing  $\text{TiO}_2$  and ZSM-5 zeolite with a Si/Al = 40 (TZ(40)) achieved the highest effi-

ciency in removal of IBU (85 %) from aqueous solution after 80 min of irradiation, through a combination of adsorption and photocatalytic degradation. The optimal condition for IBU removal in the presence of TZ(40), was natural pH (4.5), while reduced efficiency was observed at pH 7 and 10. Additionally, the removal of IBU from bottled drinking water decreased significantly (32 % removal), due to the changes of pH of reaction suspension. These findings suggest that TiO<sub>2</sub>/ZSM-5 zeolite hybrid photocatalyst could be used for the effective removal of pharmaceutical contaminates like NSAIDs IBU from aqueous environments.

#### SUPPLEMENTARY MATERIAL

Additional data and information are available electronically at the pages of journal website: <https://www.shd-pub.org.rs/index.php/JSCS/article/view/13085>, or from the corresponding author on request.

*Acknowledgements.* The authors acknowledge the financial support from the Ministry of Science, Technological Development and Innovation of the Republic of Serbia (contracts no. 451-03-65/2024-03/200146, 451-03-66/2024-03/200026, 451-03-65/2024-03/ 200161, 451-03-66/2024-03/ 200161 and 451-03-65/2024-03/200116). This research was supported by the Science Fund of the Republic of Serbia, #Grant No 7309, Project acronym: ZEOCOAT.

И З В О Д

#### УКЛАЊАЊЕ ФАРМАЦЕУТСКИ АКТИВНЕ СУПСТАНЦЕ ИБУПРОФЕНА ИЗ ВОДЕНЕ СРЕДИНЕ У ПРИСУСТВУ TiO<sub>2</sub>/ZSM-5 ЗЕОЛИТ ХИБРИДНИХ ФОТОКАТАЛИЗATORA

СРНА Ј. СТОЈАНОВИЋ<sup>1</sup>, МАРИЈА З. РИСТИЋ<sup>2</sup>, ДАНИНА Р. КРАЈИШНИК<sup>3</sup>, ВЛАДИСЛАВ А. РАЦ<sup>4</sup>  
и ЉИЉАНА С. ДАМЈАНОВИЋ-ВАСИЛИЋ<sup>1</sup>

<sup>1</sup>Универзитет у Београду – Факултет за физичку хемију, Студентски трг 12–16, 11000 Београд,

<sup>2</sup>Универзитет у Београду – ИХТМ, Центар за катализу и хемијско инжењерство, Његошева 12, 11000 Београд, <sup>3</sup>Универзитет у Београду – Фармацеутски факултет, Војводе Степе 450, 11221 Београд и

<sup>4</sup>Универзитет у Београду – Повојнорведни факултет, Немањина 6, 11080 Београд

Уклањање фармацеутски активне супстанце ибупрофена (IBU) из водене средине је испитивано у присуству TiO<sub>2</sub>/ZSM-5 зеолит хибридних фотокатализатора синтетисаних коришћењем 20 мас. % наночестичног TiO<sub>2</sub> P25 и ZSM-5 зеолита са различитим Si/Al односом (11,5, 15, 25, 40 и 140). Хибридни материјали су добијени једноставном и економски исплативом методом дисперзије у чврстој фази потпомогнутој ултразвуком, а затим карактерисани методама дифракције рендгенских зрака на праху, инфрацрвеном спектроскопијом са Фуријевом трансформацијом и дифузно рефлексионом спектроскопијом. Највећу ефикасност у уклањању IBU је показао хибридни фотокатализатор добијен од TiO<sub>2</sub> и ZSM-5 зеолита са Si/Al = 40 (ознака TZ(40)), одстрањивањем 85% IBU из воденог раствора након 80 min излагања UV зрачењу. Утврђено је да су оптимални услови за уклањање IBU из дестиљоване воде на pH 4,5, што је pH вредност воденог раствора IBU у присуству TZ(40). Додатно, испитивано је и уклањање IBU из флаширане воде за пиће у присуству TZ(40) хибридног материјала. Из раствора добијеног са флашираном водом уклоњено је само 32 % IBU, јер је промена pH реакционе сусpenзије резултовала смањењем ефикасности одстрањивања IBU.

(Примљено 18. октобра, ревидирано 9. новембра, прихваћено 1. децембра 2024)

## REFERENCES

1. A. L. Moreno Ríos, K. Gutierrez-Suarez, Z. Carmona, C. G. Ramos, L. F. Silva Oliveira, *Chemosphere* **291** (2022) 132822 (<https://doi.org/10.1016/j.chemosphere.2021.132822>)
2. Y. Li, G. Zhu, W. J. Ng, S. K. Tan, *Sci. Total Environ.* **468–469** (2014) 908 (<https://doi.org/10.1016/j.scitotenv.2013.09.018>)
3. P. Bottoni, S. Caroli, A. B. Caracciolo, *Toxicol. Environ. Chem.* **92** (2010) 549 (<https://doi.org/10.1080/02772241003614320>)
4. J. Rivera-Utrilla, M. Sánchez-Polo, M. Á. Ferro-García, G. Prados-Joya, R. Ocampo-Pérez, *Chemosphere* **93** (2013) 1268 (<https://doi.org/10.1016/j.chemosphere.2013.07.059>)
5. A. Eslami, M. M. Amini, A. R. Yazdanbakhsh, N. Rastkari, A. Mohseni-Bandpei, S. Nasseri, E. Piroti, A. Asadi, *Environ. Monit. Assess.* **187** (2015) 1 (<https://doi.org/10.1007/s10661-015-4952-1>)
6. A. Romeiro, M. E. Azenha, M. Canle, V. H. N. Rodrigues, J. P. Da Silva, H. D. Burrows, *Chem. Select* **3** (2018) 10915 (<https://doi.org/10.1002/slct.201801953>)
7. M. Petrović, B. Škrbić, J. Živančev, L. Ferrando-Climent, D. Barcelo, *Sci. Total Environ.* **468–469** (2014) 415 (<https://doi.org/10.1016/j.scitotenv.2013.08.079>)
8. J. Choina, H. Kosslick, C. Fischer, G. U. Flechsig, L. Frunza, A. Schulz, *Appl. Catal., B Environ.* **129** (2013) 589 (<https://doi.org/10.1016/j.apcatb.2012.09.053>)
9. N. Jallouli, L. M. Pastrana-Martínez, A. R. Ribeiro, N. F. F. Moreira, J. L. Faria, O. Hentati, A. M. T. Silva, M. Ksibi, *Chem. Eng. J.* **334** (2018) 976 (<https://doi.org/10.1016/j.cej.2017.10.045>)
10. D. Chen, Y. Cheng, N. Zhou, P. Chen, Y. Wang, K. Li, S. Huo, P. Cheng, P. Peng, R. Zhang, L. Wang, H. Liu, Y. Liu, R. Ruan, *J. Clean. Prod.* **268** (2020) 121725 (<https://doi.org/10.1016/j.jclepro.2020.121725>)
11. Y. Xu, C. H. Langford, *J. Phys. Chem., B* **101** (1997) 3115 (<https://doi.org/10.1021/jp962494l>)
12. M. Gar Alalm, A. Tawfik, S. Ookawara, *J. Environ. Chem. Eng.* **4** (2016) 1929 (<https://doi.org/10.1016/j.jece.2016.03.023>)
13. A. Mishra, A. Mehta, S. Basu, *J. Environ. Chem. Eng.* **6** (2018) 6088 (<https://doi.org/10.1016/j.jece.2018.09.029>)
14. Lj. Damjanovic, A. Auroux, , in *Zeolite Characterization and Catalysis*, A. W. Chester, E. G. Derouane, Eds., Springer, Dordrecht, 2009, p. 107 (<https://doi.org/10.1007/978-1-4020-9678-5>)
15. A. Grela, J. Kuc, T. Bajda, *Materials* **14** (2021) 4994 (<https://doi.org/10.3390/ma14174994>)
16. G. Hu, J. Yang, X. Duan, R. Farnood, C. Yang, J. Yang, W. Liu, Q. Liu, *Chem. Eng. J.* **417** (2021) 129209 (<https://doi.org/10.1016/j.cej.2021.129209>)
17. S. Behravesh, N. Mirghaffari, A. A. Alemajabi, F. Davar, M. Soleimani, *Environ. Sci. Pollut. Res.* **27** (2020) 26929 (<https://doi.org/10.1007/s11356-020-09038-y>)
18. K. K. Abbas, K. M. Shabeeb, A. A. A. Aljanabi, A. M. H. A. Al-Ghaban, *Environ. Technol. Innov.* **20** (2020) 101070 (<https://doi.org/10.1016/j.eti.2020.101070>)
19. S. Stojanović, M. Vranješ, Z. Šaponjić, V. Rac, V. Rakić, L. Ignjatović, L. Damjanović-Vasilić, *Int. J. Environ. Sci. Technol.* **20** (2023) 1 (<https://doi.org/10.1007/s13762-022-04305-6>)
20. T. F. Ferens, L. J. Visioli, A. T. Paulino, H. Enzweiler, *Int. J. Environ. Sci. Technol.* (2024) (<https://doi.org/10.1007/s13762-024-06076-8>)
21. N. Farhadi, T. Tabatabaei, B. Ramavandi, F. Amiri, *Ultrason. Sonochem.* **67** (2020) 105122 (<https://doi.org/10.1016/j.ultsonch.2020.105122>)

22. N. Farhadi, T. Tabatabaie, B. Ramavandi, F. Amiri, *Environ. Res.* **198** (2021) 111260 (<https://doi.org/10.1016/j.envres.2021.111260>)
23. J. Weitkamp, *Solid State Ionics* **131** (2000) 175 ([https://doi.org/10.1016/S0167-2738\(00\)00632-9](https://doi.org/10.1016/S0167-2738(00)00632-9))
24. S. Stojanović, V. Rac, K. Mojsilović, R. Vasilić, S. Marković, Lj. Damjanović-Vasilić, *Environ. Sci. Pollut. Res.* **30** (2023) 84046 (<https://doi.org/10.1007/s11356-023-28397-w>)
25. C. Baerlocher, W. M. Meier, D. H. Olson, *Atlas of Zeolite Framework Types*, 5<sup>th</sup> ed., Elsevier, Amsterdam, Holland, 2001 ([https://www.iza-structure.org/books/Atlas\\_5ed.pdf](https://www.iza-structure.org/books/Atlas_5ed.pdf))
26. H. G. Karge, E. Geidel, in *Characterization I. Molecular Sieves – Science and Technology*, Vol. 4, H. G. Karge, J. Weitkamp, Eds., Springer, Berlin, 2004, p. 1 (ISBN: 978-3-54-064335-7)
27. J. G. Yu, H.G. Yu, B. Cheng, X-J. Zhao, J. C. Yu, W-K. Ho, *J. Phys. Chem., B* **107** (2003) 13871 (<https://doi.org/10.1021/jp036158y>)
28. A. N. Ökte, Ö. Yilmaz, *Appl. Catal., A* **354** (2009) 132 (<https://doi.org/10.1016/j.apcata.2008.11.022>)
29. N. Jiang, R. Shang, S.G.J. Heijman, L.C. Rietveld, *Water Res.* **144** (2018) 145 (<https://doi.org/10.1016/j.watres.2018.07.017>)
30. X. Zhang, F. Wu, X.W. Wu, C. Pengyu, D. Nansheng, *J. Hazard. Mater.* **157** (2008) 300 (<https://doi.org/10.1016/j.jhazmat.2007.12.098>)
31. U. I. Gaya, A. H. Abdullah, *J. Photochem. Photobiol., C* **9** (2008) 1 (<https://doi.org/10.1016/j.jphotochemrev.2007.12.003>)
32. D. Krajišnik, A. Daković, A. Malenović, M. Kragović, J. Milić, *Clay Miner.* **50** (2015) 11 (<https://doi.org/10.1180/claymin.2015.050.1.02>)
33. P. Iovino, S. Canzano, S. Capasso, A. Erto, D. Musmarra, *Chem. Eng. J.* **277** (2015) 360 (<https://doi.org/10.1016/j.cej.2015.04.097>)
34. H. Ding, J. Hu, *Chem. Eng. J.* **397** (2020) 125462 (<https://doi.org/10.1016/j.cej.2020.125462>)
35. N. Negishi, Y. Miyazaki, S. Kato, Y. Yang, *Appl. Catal., B* **242** (2019) 449 (<https://doi.org/10.1016/j.apcatb.2018.10.022>).